A Subclass of bHLH Proteins Required for Cardiac Morphogenesis

Deepak Srivastava,* Peter Cserjesi,† Eric N. Olson‡

Skeletal muscle development is controlled by a family of muscle-specific basic helix-loop-helix (bHLH) transcription factors. Two bHLH genes, *dHAND* and *eHAND*, have now been isolated that are expressed in the bilateral heart primordia and subsequently throughout the primitive tubular heart and its derivatives during chick and mouse embryogenesis. Incubation of stage 8 chick embryos with *dHAND* and *eHAND* antisense oligonucleotides revealed that either oligonucleotide alone had no effect on embryonic development, whereas together they arrested development at the looping heart tube stage. Thus, *dHAND* and *eHAND* may play redundant roles in the regulation of the morphogenetic events of vertebrate heart development.

Congenital malformations of the heart occur in about 8 per 1000 live births in humans and among stillbirths may be up to 10 times as frequent (*1*). Heart formation during vertebrate embryogenesis involves the commitment of mesodermal precursor cells to the cardiac lineage and the subsequent formation of a primitive heart tube, which, in turn, undergoes looping, formation of the outflow tract and atrial and ventricular cavities, and septation to form the mature four-chambered heart. Little is known of the underlying genetic pathways that control cardiac morphogenesis.

Members of the bHLH family of transcription factors regulate skeletal myogenesis (*2, 3*), neurogenesis (*4*), and hematopoiesis (*5*). Dimerization of bHLH proteins mediated by the HLH motif results in juxtaposition of their basic regions and formation of a bipartite DNA-binding domain that recognizes the E-box consensus sequence (CANNTG) in the control regions of downstream target genes. Although skeletal and cardiac muscle express many of the same muscle-specific genes, skeletal muscle bHLH proteins are not expressed in the heart. However, indirect evidence suggests that bHLH proteins may participate in the control of cardiac muscle gene expression (*6–10*).

We recently described a bHLH protein, termed eHAND, that is expressed in the heart, the extraembryonic membranes, and several neural crest derivatives during mouse embryogenesis (*11*). Because bHLH proteins often belong to families, we screened mouse genomic and embryonic complementary DNA (cDNA) libraries under conditions of reduced stringency with the bHLH region of the *eHAND* cDNA as a probe to identify closely related genes (*12*). Several clones that represented an *eHAND*-related gene were isolated. The longest cDNA contained 1130 base pairs, with an AUG codon preceding an open reading frame that potentially encoded a 217–amino acid protein (Fig. 1A) (*13*). The *eHAND*-related gene was named *dHAND*, because it is expressed in the deciduum, heart, autonomic nervous system, and neural crest derivatives. The deduced open reading frame of the dHAND protein contains a bHLH region that is 87% identical to that of eHAND (Fig. 1, A and B) (*14*).

The expression pattern of *dHAND* transcripts during embryogenesis was determined by in situ hybridization of mouse embryo sections (*15*). At 7.5 days postcoitum (p.c.), *dHAND* was expressed at high levels in the maternally derived deciduum (*16*), but expression was not detected in the embryo or in the extraembryonic membranes. In contrast, *eHAND* is not expressed in the deciduum but is expressed at high levels in extraembryonic membranes (*11*). Within the embryo, we first detected *dHAND* expression in the lateral mesoderm on day 7.75 p.c. (*16*). On day 8.5 p.c., *dHAND* expression was apparent throughout the developing heart (Fig. 2, A to D); the abundance of transcripts in the bulbus cordis and aortic sac was greater than that in the future left ventricle (Fig. 2, A and B). In the caudal region of the embryo, *dHAND* was expressed in the lateral mesoderm at the level of separation of the somatic and splanchnic mesoderm (Fig. 2, C and D).

On day 9.5 p.c., *dHAND* was expressed throughout the developing cardiovascular region, with transcripts most abundant in the outflow tract (truncus arteriosus) and in the first and second aortic arch arteries (Fig. 2, E and F). On day 10.5 p.c., *dHAND* transcripts were abundant in the first branchial arch as well as in the truncus arteriosus, aortic sac, and third and fourth aortic arches (*16*). All of these structures are populated by neural crest cells (*17*). The expression of *dHAND* was less marked in the mesoderm-derived ventricle, atrium, sinus venosus, and cardinal veins. Later in development, on day 13.5 p.c., *dHAND* expression was barely detectable in the heart, but was apparent in the neural crest–derived sympathetic trunk and adrenal medulla, similar to the expression pattern of *eHAND* (*16*). After day 16 p.c., *dHAND* expression decreased throughout the embryo to levels that were not readily detectable by in situ hybridization (*16*).

The early events of cardiogenesis have been studied in greatest detail in the chick, in which cells from the anterior lateral plate mesoderm become committed to the cardiogenic lineage at approximately stage 4 (*18*). Subsequent fusion of the bilateral cardiac primordia gives rise to the primitive heart tube and initiation of the rhythmic heart beat at stage 10. The heart then undergoes looping, followed by the appearance of atria and ventricles. To define further the expression patterns of *dHAND* and *eHAND* and to begin to determine their functions, we isolated cDNAs for the corresponding chicken genes. By low-stringency screening of a chick embryo cDNA library (*12*), we identified two groups of clones that appeared to encode dHAND and eHAND homologs, respectively. The predicted mouse dHAND protein was 96% identical to the putative chick dHAND (Fig. 1C), whereas chick and mouse eHAND showed 73% identity. We have no evidence for additional chick genes with homology to *dHAND* and *eHAND*.

The expression patterns of the chick genes were analyzed by whole-mount in situ hybridization (*19*). Expression of *dHAND* was first detected at stage 8$^-$ of Hamburger and Hamilton (*20*) in the lateral mesoderm and the precardiogenic mesoderm (Fig. 3A); *eHAND* expression was detected slightly later at stage 8 in the cardiac crescent (Fig. 3E). Both genes were expressed in the cardiac crescent and fusing heart tubes at stage 9 (Fig. 3, B and F). At stage 10, the paired heart primordia have fused to form a single contracting heart tube; *dHAND* and *eHAND* were expressed throughout the cardiac tube and the sinus venosus, which is the venous inflow to the heart (Fig. 3, C and G). By stage 15, when the heart tube has looped, both genes continued to be expressed homogeneously in the various regions of the heart, including the atria, future left ventricle, bulbus cordis, and truncus arteriosus (Fig. 3, D and H). Both *dHAND* and *eHAND* were also expressed throughout the branchial arches, which begin forming at this stage. Expression of both genes persisted through stage 20, but decreased thereafter. The temporospatial expression patterns of *dHAND* and *eHAND*

Department of Biochemistry and Molecular Biology, The University of Texas M. D. Anderson Cancer Center, Houston, TX 77030, USA.

*Present address: Departments of Pediatrics (Division of Cardiology) and Molecular Biology and Oncology, The University of Texas Southwestern Medical Center, Dallas, TX 75235, USA.
†Present address: Department of Anatomy and Cell Biology, Columbia University, New York, NY 10032, USA.
‡Present address: Department of Molecular Biology and Oncology, The University of Texas Southwestern Medical Center, Dallas, TX 75235, USA.

were similar during chick and mouse embryogenesis (*16*), suggesting that the functions of these genes may also be conserved across species.

To determine the functions of the *HAND* genes, we used antisense oligonucleotides specific to *dHAND* and *eHAND* transcripts to prevent their expression in early chick embryos as was previously achieved for the zinc finger gene *Slug* (*21*). Embryos were isolated at stage 8, incubated for 30 min in yolk-Tyrode's solution (*22*) containing antisense oligonucleotides, laid ventral side up on albumin agar, and grown in vitro at 38.5°C as described (*23*). An additional drop of solution containing 80 μM oligonucleotide was added directly to the embryo every 4 hours and cardiogenesis was monitored visually. Under these culture conditions, control embryos survived for at least 2 days and underwent normal development through at least stage 20. Throughout this time, the embryos exhibited a rhythmic heart beat comparable to that of embryos in situ.

We used two different antisense oligonucleotides for both *dHAND* and *eHAND* that were selected on the basis of both the predicted stability of the RNA:DNA duplex, which correlates with susceptibility to hydrolysis by ribonuclease H (*24*), and the absence of related sequences in databases, to prevent annealing of the oligonucleotides to other transcripts. We also chose antisense sequences that would be specific to either *dHAND* or *eHAND* transcripts and would not hybridize to both. The oligonucleotides were synthesized as phosphorothioate derivatives to protect against degradation by nucleases (*25*). No single antisense oligonucleotide had an effect on cardiac development when added at a concentration of 80 μM (Table 1). However, combination of antisense oligonucleotides for *dHAND* and *eHAND* at concentrations of 40 μM each resulted in arrest of heart development at stage 11 to 12, when cardiac looping occurs. Treatment with antisense oligonucleotides that corresponded to two different regions of *dHAND* and *eHAND* transcripts produced identical effects. A similar effect was apparent with combinations of oligonucleotides at concentrations of 20 μM each, but embryos were unaffected at concentrations of <10 μM. Random oligonucleotides with the same base composition as the antisense oligonucleotides had no effect on development.

At stage 11 to 12, at which chick embryos were arrested by *dHAND* and *eHAND* antisense oligonucleotides, the heart had begun to undergo rightward looping, and the primitive atrial and ventricular chambers had started to become demarcated; however, valves and trabeculae had not yet started to form. Whereas control embryos developed normally through this stage, the arrested embryos exhibited a sluggish heartbeat, became distended, and developed pericardial edema. These defects suggest that the affected embryos died from hemodynamic insufficiency.

The observation that development was arrested only in the presence of both *dHAND* and *eHAND* oligonucleotides suggests that the effects were specific and that the two genes might perform redundant functions. The ability of oligonucleotides targeted to different sequences in the *dHAND* and

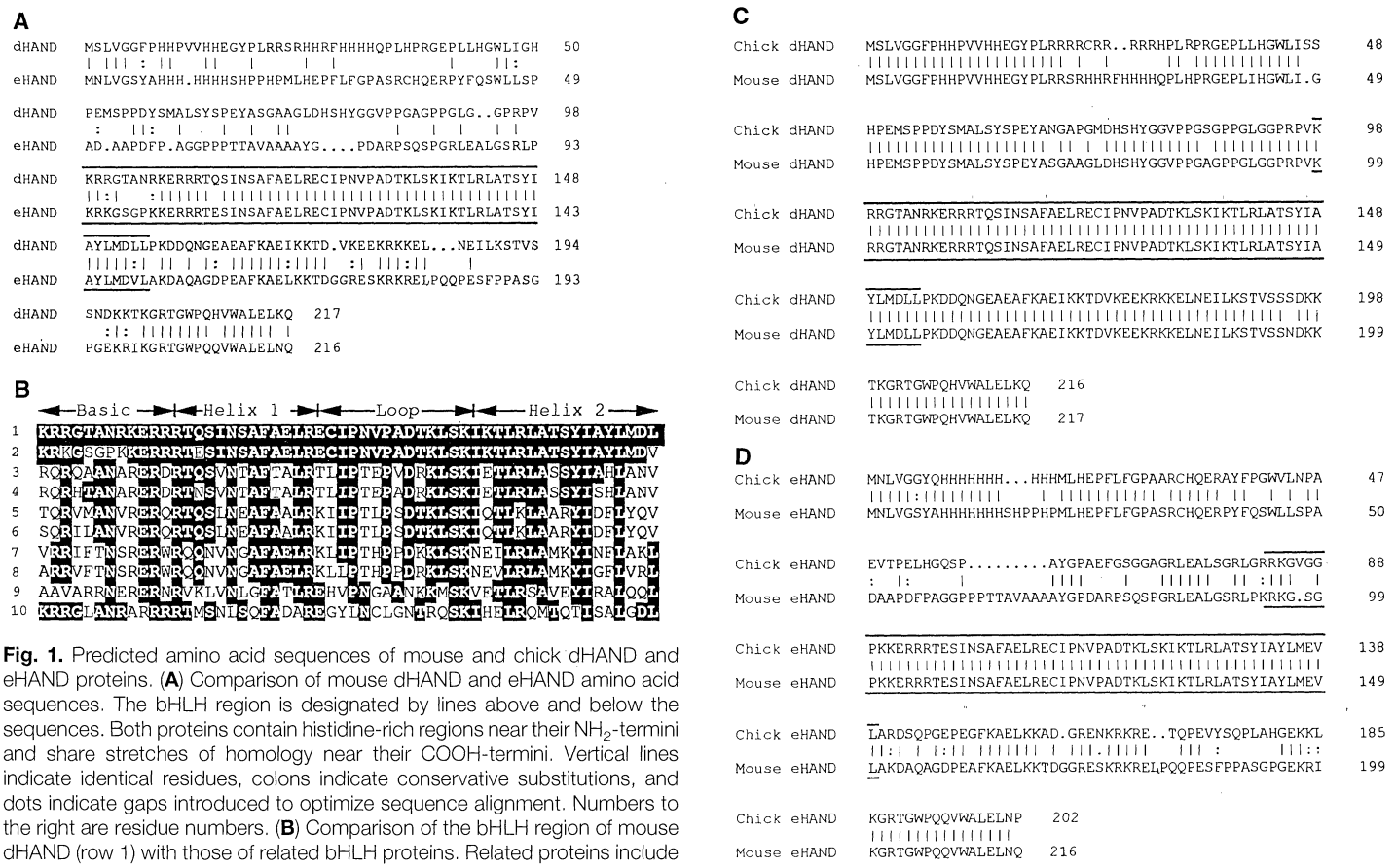

Fig. 1. Predicted amino acid sequences of mouse and chick dHAND and eHAND proteins. (**A**) Comparison of mouse dHAND and eHAND amino acid sequences. The bHLH region is designated by lines above and below the sequences. Both proteins contain histidine-rich regions near their NH_2-termini and share stretches of homology near their COOH-termini. Vertical lines indicate identical residues, colons indicate conservative substitutions, and dots indicate gaps introduced to optimize sequence alignment. Numbers to the right are residue numbers. (**B**) Comparison of the bHLH region of mouse dHAND (row 1) with those of related bHLH proteins. Related proteins include eHAND (row 2); Paraxis (row 3), also termed bHLH-EC2 and Meso-1, which is expressed in paraxial mesoderm and somites (*30*); mouse Scleraxis (row 4), which is expressed in mesenchymal precursors of the skeleton (*29*); mouse Twist (row 5) (*31*), which is expressed in mesoderm and neural crest cells; mouse Dermo-1 (row 6) (*32*), which is highly expressed in developing dermis; the hematopoietic proteins SCL-1 (row 7) (*33*) and Lyl-1 (row 8) (*34*); and MASH-1 (row 9) (*35*), which is expressed in the central and peripheral nervous system. The basic region of dHAND is most closely related to that of Atonal (row 10), which regulates neurogenesis in *Drosophila* (*36*). Identical residues are shown in white on black. (**C** and **D**) Comparison of mouse and chick dHAND (C) and eHAND (D) sequences. Abbreviations for the amino acid residues are A, Ala; C, Cys; D, Asp; E, Glu; F, Phe; G, Gly; H, His; I, Ile; K, Lys; L, Leu; M, Met; N, Asn; P, Pro; Q, Gln; R, Arg; S, Ser; T, Thr; V, Val; W, Trp; and Y, Tyr.

eHAND transcripts to arrest cardiac morphogenesis and the absence of an effect of random oligonucleotides also indicated that the effects were specific.

To investigate further the specificity of the antisense effects, we examined the expression of *HAND* gene transcripts by whole-mount in situ hybridization (Fig. 4). In the presence of a specific antisense oligonucleotide, the corresponding mRNA was not detected (Fig. 4, C and F), whereas the mRNA from the other gene was detected in normal amounts (Fig. 4, B and G). However, in the presence of antisense oligonucleotides targeted to both genes, neither *dHAND* nor *eHAND* mRNAs were detected (Fig. 4, D and H).

We also examined the expression of transcripts encoding the cardiac transcription factor MEF2C (*26*) or cardiac α-actin in embryos to determine whether the *HAND* gene antisense oligonucleotides had a general inhibitory effect on differentiation of cardiac myocytes. Until the time at which heart development was arrested, there was no detectable difference in the patterns of expression of cardiac α-actin (Fig. 4, I to L) or MEF2C (*16*) transcripts among embryos exposed to the different oligonucleotides.

Cardiac looping is thought to occur as a result of cellular proliferation and specific interactions with extracellular matrix molecules (*27*). The most likely explanation of the synchronous arrest of development in the presence of *dHAND* and *eHAND* antisense oligonucleotides is that *dHAND* and *eHAND* regulate one or more genes required for cardiac looping and that, in the absence of the encoded proteins, looping is arrested and is associated with poor hemodynamic performance and embryonic death. Resolution of the precise cause of arrested cardiac development will require identification of the specific target genes of the HAND proteins. Because early embryonic cardiac defects can be difficult to analyze in mice, the use of antisense oligonucleotides in avian embryos may facilitate analysis of early genetic events associated with cardiac morphogenesis.

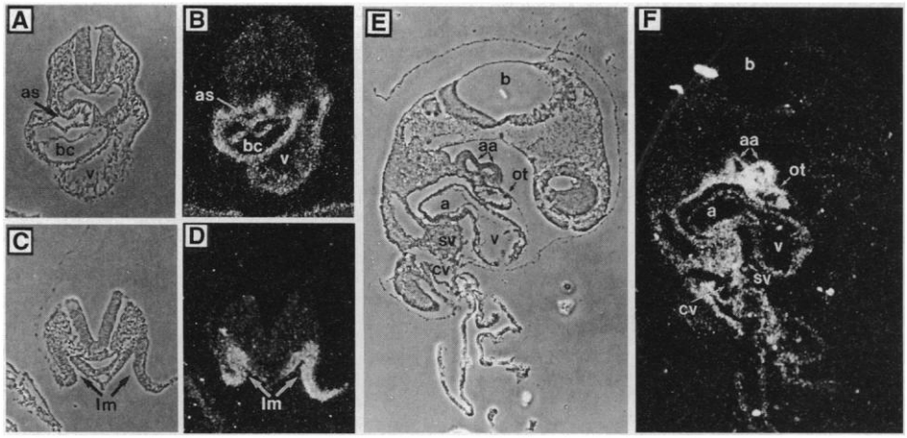

Fig. 2. Expression of *dHAND* transcripts in mouse embryos. Transverse and saggital sections of mouse embryos on days 8.5 (**A** to **D**) and 9.5 (**E** to **F**) p.c. were examined for *dHAND* expression by in situ hybridization. Sections in (A) to (D) passed through the embryo twice. Rostral sections of the embryo (A and B) demonstrated *dHAND* expression in the bulbus cordis (bc), ventricle (v), and aortic sac (as). Caudal sections (C and D) revealed *dHAND* expression in the somatic and splanchnic lateral mesoderm (lm). On day 9.5 p.c., *dHAND* transcripts were most abundant in the first and second aortic arches (aa) and the cardiac outflow tract (ot), but were also present in the atrium (a), ventricles (v), sinus venosus region (sv), and cardinal vein (cv); b, brain (E and F). (A), (C), and (E) are phase-contrast images.

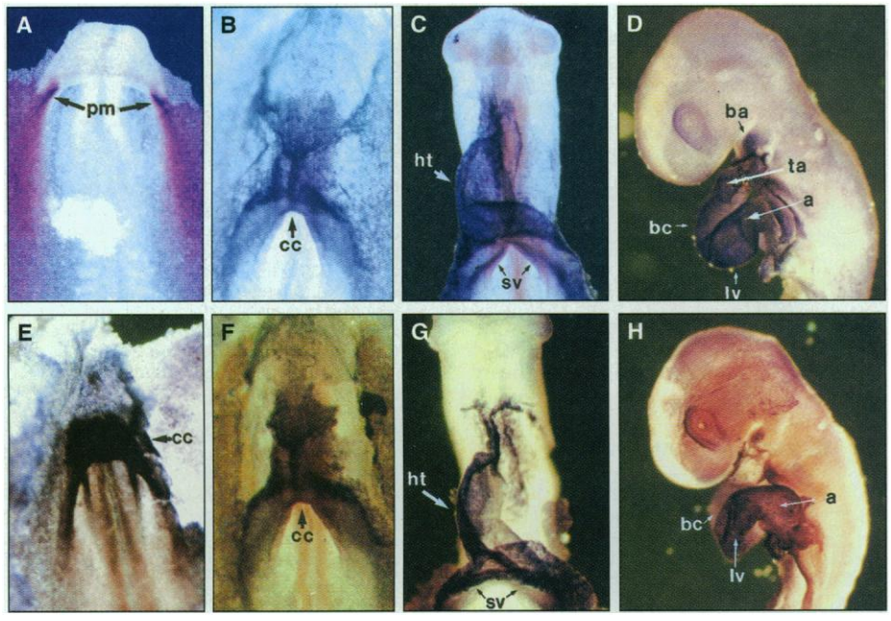

Fig. 3. Expression of *dHAND* and *eHAND* in chick embryos. Transcripts of *dHAND* (**A** to **D**) and *eHAND* (**E** to **H**) were detected in chick embryos by whole-mount in situ hybridization. Expression of *dHAND* was first detected in the precardiogenic mesoderm (pm) at stage 8⁻ (A), whereas *eHAND* transcripts were detected slightly later in the cardiac crescent (cc) at stage 8 (E). At stage 9, both *dHAND* (B) and *eHAND* (F) were expressed in the cardiac crescent and the paired heart tubes as they were fusing. Stage 10 embryos showed expression of *dHAND* (C) and *eHAND* (G) throughout the heart tube (ht) and the sinus venosus (sv). Expression of *dHAND* in the stage 16 (D) embryo was apparent in the truncus arteriosus (ta), bulbus cordis (bc), future left ventricle (lv), atria (a), and branchial arch (ba). A similar pattern of expression was observed for *eHAND* in a stage 15 embryo (H).

Table 1. Effects of *HAND* gene antisense oligonucleotides on heart development. Stage 8 chick embryos were isolated and incubated in vitro in the presence of the indicated oligonucleotides (80 μM) (*21*). Values represent the number of embryos that were unaffected or showed arrest of cardiac development after 48 hours; arrest was apparent at 18 to 20 hours; (1) and (2) refer to two different antisense oligonucleotides for both *dHAND* and *eHAND* sequences. Whereas no single oligonucleotide had a significant effect on cardiac development, most embryos exposed to both *dHAND* and *eHAND* antisense oligonucleotides showed arrested cardiac development at stage 11 to 12 ($P < 0.0001$, Fisher's exact test), during cardiac looping.

Oligonucleotide	No. of embryos unaffected	No. of embryos arrested at cardiac looping stage
dHAND(1)	10	0
dHAND(2)	9	1
eHAND(1)	10	0
eHAND(2)	9	1
dHAND(1) + eHAND(1)	4	14
dHAND(2) + eHAND(2)	4	11
Random	23	1

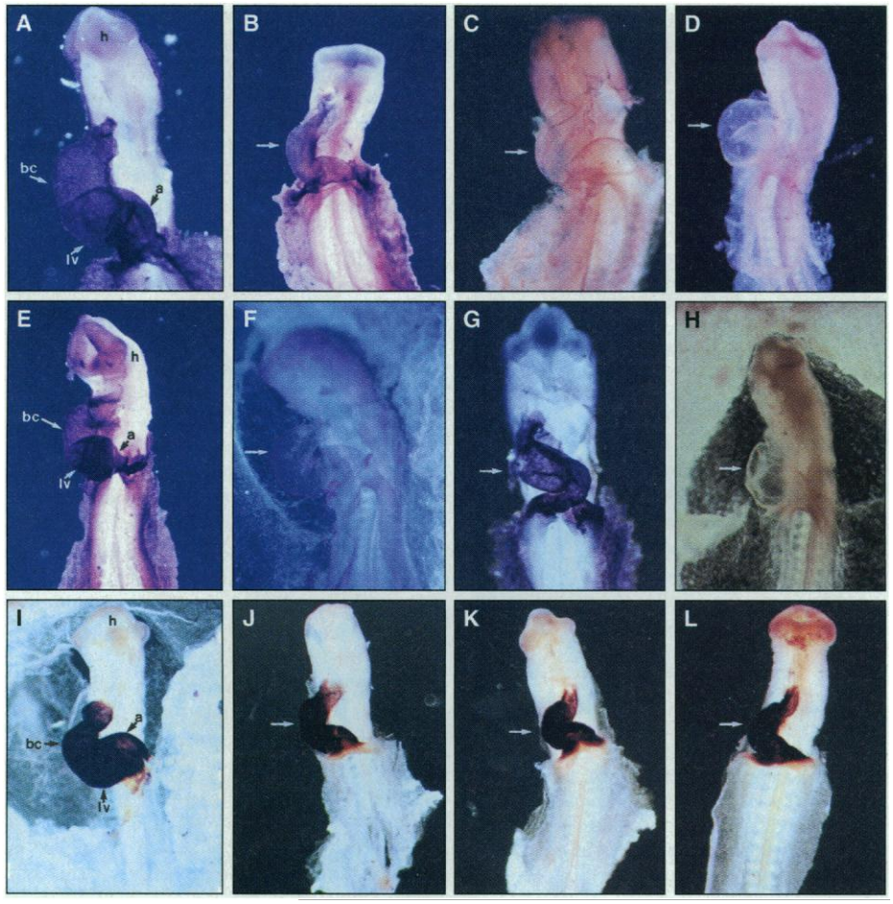

Fig. 4. Expression of *dHAND* and *eHAND* in chick embryos exposed to antisense oligonucleotides. Transcripts of *eHAND* (**A** to **D**), *dHAND* (**E** to **H**), and cardiac α-actin (**I** to **L**) were detected by in situ hybridization in embryos exposed to various oligonucleotides. Expression of *eHAND* was detected in embryos exposed to random (A) and *dHAND* antisense (B) oligonucleotides, but not in those exposed to *eHAND* (C) or a combination of *dHAND* and *eHAND* (D) antisense oligonucleotides. Similarly *dHAND* mRNA was detected in normal amounts in embryos incubated with random (E) or *eHAND* antisense (G) oligonucleotides, but not in those incubated with *dHAND* (F) or both *dHAND* and *eHAND* (H) antisense oligonucleotides. The cardiac α-actin gene was expressed normally in embryos exposed to random (I), *dHAND* (J), *eHAND* (K), or *dHAND* plus *eHAND* (L) antisense oligonucleotides. h, head; bc, bulbus cordis; lv, left ventricle; a, atria. Unlabeled arrows indicate region of heart.

The cardiovascular system is derived largely from lateral mesoderm and neural crest cells, in which the *HAND* genes are expressed at high levels. Ablation of the cardiac neural crest in chick embryos results in a variety of cardiac defects, with a predominance of truncal defects, such as persistent truncus arteriosus, tetralogy of Fallot, and double-outlet right ventricle, as well as aortic arch anomalies (*17*). Many of these defects are similar to those apparent in DiGeorge–CATCH-22 syndrome, which is thought to be related to abnormal neural crest development. The coincident expression of the *HAND* genes in those tissues composed in part of the circumpharyngeal neural crest suggests a possible role for these genes in the normal development of the conotruncus and aortic arch as well as certain other neural crest–derived tissues. Defects in looping also appear to contribute to several congenital heart defects in humans (*28*). It will be of interest to determine whether mutations in *dHAND* or *eHAND* contribute to human congenital heart anomalies.

REFERENCES AND NOTES

1. J. I. E. Hoffman, *Pediatr. Cardiol.* **16**, 103 (1995).
2. E. N. Olson and W. H. Klein, *Genes Dev.* **8**, 1 (1994).
3. H. Weintraub, *Cell* **75**, 1241 (1993); M. A. Rudnicki and R. Jaenisch, *Bioessays* **17**, 203 (1995).
4. L. Y. Jan and L. N. Jan, *Cell* **75**, 827 (1993); J. E. Lee *et al.*, *Science* **268**, 836 (1995).
5. Y. Zhuang, P. Soriano, H. Weintraub, *Cell* **79**, 875 (1994); G. Bain *et al.*, *ibid.*, p. 885; R. A. Shivdasani, E. L. Mayer, S. H. Orkin, *Nature* **373**, 432 (1995).
6. E. N. Olson, *Circ. Res.* **72**, 1 (1993); V. Sartorelli, M. Kurabayashi, L. Kedes, *ibid.*, p. 925.
7. V. Sartorelli, N. A. Hong, N. H. Bishopric, L. Kedes, *Proc. Natl. Acad. Sci. U.S.A.* **89**, 4047 (1992).
8. S. Navankasattusas, M. Sawadogo, M. van Bilsen, C. Dang, K. R. Chien, *Mol. Cell. Bio.* **14**, 7331 (1994); J. D. Molkentin, R. S. Brogan, S. M. Jobe, B. E. Markham, *J. Biol. Chem.* **268**, 2602 (1993).
9. J. P. Springhorn, O. Ellingen, H. Berger, R. A. Kelly, T. W. Smith, *J. Biol. Chem.* **267**, 14360 (1992); S. M. Evans, B. A. Walsh, C. B. Newton, *Circ. Res.* **73**, 569 (1993); S. M. Evans and T. X. O'Brien, *Dev. Biol.* **159**, 485 (1993).
10. J. Litvin, M. O. Montgomery, D. J. Goldhammer, C. P. Emerson, D. M. Bader, *Dev. Biol.* **156**, 409 (1993).
11. P. Cserjesi, D. Brown, G. E. Lyons, E. N. Olson, *ibid.* **170**, 664 (1995).
12. To search for *eHAND*-related genes, we screened a mouse genomic library, constructed in phagemids (lambda 129), with a ^{32}P-labeled Stu I–Sty I restriction fragment of the *eHAND* cDNA (*11*). This probe comprised 741 nucleotides and included the bHLH region. Two genomic equivalents were screened under conditions of low stringency. Hybridizations were performed ovemight at 42°C in 6× SSPE [1× SSPE: 150 mM NaCl, 10 mM NaH_2PO_4, 1 mM EDTA (pH 7.4)] containing 0.5% SDS, 30% formamide, and salmon sperm DNA (100 μg/ml). Filters were washed in 2× SSC [1× SSC: 150 mM NaCl, 15 mM sodium citrate (pH 7.0)] containing 0.1% SDS for 20 min at room temperature and then for 15 min at 50°C. Positive clones were purified and analyzed by Southern (DNA) blots and the polymerase chain reaction. Clones of interest were subcloned into plasmid vectors (Bluescript SK) and sequenced. Sequence analysis was performed with the GCG sequence analysis software package. The mouse *dHAND* cDNA was isolated by screening a 12.5-day postcoitum mouse embryo cDNA library with a ^{32}P-labeled 112–base pair polymerase chain reaction product from the region immediately 3′ of the bHLH domain of a new genomic clone (nucleotides 520 to 631 of cDNA). Hybridization was performed under high-stringency conditions at 42°C in 6× SSPE containing 0.5% SDS, 50% formamide, and salmon sperm DNA (100 μg/ml). Filters were washed twice at 65°C in 0.1× SSC containing 0.1% SDS. Clones of interest were purified, excised into plasmid vectors, and sequenced. Chicken *dHAND* and *eHAND* cDNAs were isolated by screening a stage 12 chick embryo cDNA library with a ^{32}P-labeled fragment of mouse *dHAND* cDNA that included the bHLH region (nucleotides 292 to 644). Hybridization was performed under conditions of low stringency as described above. Clones were purified, excised into plasmid vectors, and sequenced.
13. The nucleic acid sequences have been deposited with GenBank. The accession numbers for mouse *dHAND*, chick *dHAND*, and chick *eHAND* are U40039, U40040, and U40041, respectively.
14. After submission of this paper, mouse *dHAND* and *eHAND* were cloned and characterized by other groups and were termed *Thing-1* and *Thing-2* [S. M. Hollenberg *et al.*, *Mol. Cell. Biol.* **15**, 3813 (1995)] and *Hxt* and *Hed* [J. C. Cross *et al.*, *Development* **121**, 2513 (1995)], respectively.
15. In situ hybridization to mouse embryo sections was performed with ^{35}S-labeled RNA probes (*26*). Antisense RNA probes were synthesized with T7 and Sp6 RNA polymerases from a subclone of *dHAND* spanning nucleotides 292 to 644 and from full-length cDNA, respectively. Hybridization was performed on tissue sections of mouse embryos ranging from 7.5 days p.c. to term. After hybridization, sections were washed and dipped in Kodak NTB-2 emulsion. Slides were exposed for 7 days and then developed in D19 (Kodak) for 3 min.
16. D. Srivastava and E. N. Olson, unpublished observations.
17. M. L. Kirby and K. L. Waldo, *Circulation* **82**, 332 (1990).
18. J. Litvin, M. Montgomery, A. Gonzalez-Sanchez, J. G. Bisaha, D. Bader, *Trends Cardiovasc. Med.* **2**, 27 (1992).
19. J. Barth and R. Ivarie, *BioTechniques* **17**, 324 (1994). In situ hybridization of chick embryos was performed with digoxygenin-labeled RNA probes synthesized with T7 polymerase from full-length chick *dHAND* and *eHAND* cDNAs.
20. V. Hamburger and H. Hamilton, *J. Morphol.* **88**, 49 (1951).
21. M. A. Nieto, M. G. Sargent, D. G. Wilkinson, J. Cooke, *Science* **264**, 835 (1994).
22. Egg yolk was collected and mixed 1:1 with Tyrode's solution [100 mM NaCl, 10 mM Na_2HPO_4, 2 mM KCl, 0.8 mM $MgCl_2$, 0.75 mM $CaCl_2$, 8.3 mM glu-

cose (pH 7.25)]. The mixture was centrifuged at 10,000*g* for 10 min, and the supernatant was diluted 1:10 with Tyrode's solution. Oligonucleotides were added to a final concentration of 80 μM. Embryos were incubated with the following antisense oligonucleotides: dHAND (1), CCCGTTCTGGTCGTCCTTG; eHAND (1), CTCCGTTCTCCTCCTCTCC; dHAND (2), ACTCGGGGCTGTAGGAC; or eHAND (2), TCCTCCCGAACCGAGCTC. Random oligonucleotides were also synthesized with a base composition similar to that of the antisense oligonucleotides.

23. G. C. Schoenwolf and R. L. Watterson, *Laboratory Studies of the Chick, Pig, and Frog Embryos* (Macmillan, New York, 1989).
24. R. W. Wagner, *Nature* **372**, 333 (1994).
25. G. Zon and W. J. Stec, in *Oligonucleotides and Analogues*, F. Eckstein, Ed. (Oxford Univ. Press, Oxford, 1991), pp. 87–108.
26. D. G. Edmondson, G. E. Lyons, J. F. Martin, E. N. Olson, *Development* **120**, 1251 (1994).
27. W. J. Yost, *Cell* **82**, 689 (1995).
28. R. M. Payne, M. C. Johnson, J. W. Grant, A. W. Strauss, *Circulation* **91**, 494 (1995).
29. P. Cserjesi *et al.*, *Development* **121**, 1099 (1995).
30. R. Burgess, P. Cserjesi, K. L. Ligon, E. N. Olson, *Dev. Biol.* **168**, 296 (1995); E. E. Quertermous, H. Hidai, M. A. Blanar, T. Quertermous, *Proc. Natl. Acad. Sci. U.S.A.* **91**, 7066 (1994); M. Blanar *et al.*, *ibid.* **92**, 5870 (1995).
31. C. Wolf, C. Thisse, B. Stoetzel, P. Gerlinger, F. Perrin-Schmitt, *Dev. Biol.* **142**, 363 (1991).
32. L. Li, P. Cserjesi, E. N. Olson, *ibid.* **172**, 280 (1995).
33. C. G. Begley *et al.*, *Proc. Natl. Acad. Sci. U.S.A.* **88**, 869 (1991).
34. J. D. Mellentin, S. D. Smith, M. L. Cleary, *Cell* **58**, 77 (1989).
35. J. E. Johnson, S. J. Birren, D. J. Anderson, *Nature* **346**, 858 (1990).
36. A. P. Jarman, Y. Grau, L. Y. Jan, Y. N. Jan, *Cell* **73**, 1307 (1993).

37. We thank M. Chase for assistance with DNA sequencing, K. Tucker for editorial assistance, and A. Tizenor for assistance with graphics. Supported by grants from NIH, the Muscular Dystrophy Association, and the Robert A. Welch Foundation to E.N.O. D.S. was supported by a fellowship from the NIH Pediatric Scientist Development Program.

28 June 1995; accepted 28 September 1995

The ARF1 GTPase-Activating Protein: Zinc Finger Motif and Golgi Complex Localization

Edna Cukierman, Irit Huber, Miriam Rotman, Dan Cassel*

Hydrolysis of guanosine triphosphate (GTP) by the small guanosine triphosphatase (GTPase) adenosine diphosphate ribosylation factor-1 (ARF1) depends on a GTPase-activating protein (GAP). A complementary DNA encoding the ARF1 GAP was cloned from rat liver and predicts a protein with a zinc finger motif near the amino terminus. The GAP function required an intact zinc finger and additional amino-terminal residues. The ARF1 GAP was localized to the Golgi complex and was redistributed into a cytosolic pattern when cells were treated with brefeldin A, a drug that prevents ARF1-dependent association of coat proteins with the Golgi. Thus, the GAP is likely to be recruited to the Golgi by an ARF1-dependent mechanism.

The budding of transport vesicles from the Golgi compartment requires the association of cytoplasmic coat proteins with the organelle membrane. The small GTP-binding protein ARF1 acts as a key regulator of the interactions of nonclathrin coat protein (coatomer) with Golgi stacks (*1*) and of clathrin adaptor particles with the trans-Golgi network (*2*). Like other GTP-binding proteins, ARF1 exerts its regulatory effect by virtue of its GTPase cycle (*3*). In its GTP-bound form, ARF1 triggers the association of coat protein with the Golgi membrane. The subsequent hydrolysis of ARF1-bound GTP is required for the dissociation of coat protein from Golgi membranes and vesicles (*4*). The ARF1 protein also functions as a regulator of the enzyme phospholipase D (*5*), and a possible relation between this role of ARF1 and its function in membrane traffic has been proposed (*6*). The fact that pure ARF1 is unable to hydrolyze GTP (*7*) suggests the existence of an ARF1-directed GAP. Because GTP hydrolysis on ARF1 is required for coat protein dissociation, an ARF1 GAP is likely to function in the uncoating of Golgi-derived vesicles that must take place before their fusion with the target membrane.

We recently purified a 49-kD ARF1 GAP from rat liver cytosol (*8*). Polymerase chain reaction (PCR) amplification of complementary DNA (cDNA) with degenerate primers based on amino acid sequences of this protein generated a 0.5-kb fragment. Screening of a rat liver cDNA library with this fragment as a probe yielded several positive clones. Alignment of the sequences of two overlapping clones (Z6 and G11) revealed an entire open reading frame flanked by 5′ and 3′ untranslated regions (Fig. 1A). The coding sequence predicts a protein of 415 amino acids (45,448 daltons) that includes all peptides that we have sequenced from the tissue-purified protein. The initiating methionine conforms with the Kozak rules for the initiation of translation (*9*) and is preceded 267 nucleotides upstream by an in-frame stop codon.

Department of Biology, Technion–Israel Institute of Technology, Haifa 32000, Israel.

*To whom correspondence should be addressed. E-mail: bir06dc@technion.technion.ac.il

Analysis of the primary structure of the GAP revealed a hydrophilic protein with multiple potential phosphorylation sites of protein kinase C. Although the ARF1 GAP does not show similarity to other GAPs, it shows a high degree of similarity to *Saccharomyces cerevisiae* proteins (*10*) designated Gcs1p, Glo3p, and Sps18p (48, 46, and 33% identity, and 70, 70, and 60% similarity, including evolutionarily conserved substitutions, respectively). An even higher similarity exists between the NH_2-terminal parts of the proteins (Fig. 1B). A common feature of the GAP and the yeast proteins is the presence near their NH_2-termini of a conserved $CXXCX_{16}CXXC$ motif (where X is any amino acid), which apparently represents a zinc finger structure (*10*). Additional proteins that contain some of the conserved sequences shown in Fig. 1B, including the zinc finger domain, are presented in databank entries from humans, nematodes, and plants.

In addition to clone Z6, which appears to encode the tissue-purified protein, we isolated from the rat liver library two clones that are likely to represent alternative splice variants (Fig. 2A). One variant (W15) had a deletion of 110 base pairs (bp) near the 5′ end of the coding region, including the putative zinc finger domain. Although the initiation codon is not removed by the deletion, this codon cannot be used for translation in clone W15 because of a frame shift that generates an early stop codon. However, the W15 variant may be translated from a second in-frame methionine.

A second variant (Z5) contained a 0.6-kb insert within the codon for amino acid 278 (Fig. 2A). Only five insert-derived amino acids are added before a new stop codon is encountered, predicting a truncated protein of 31 kD. The presence of the Z5 variant in rat liver cDNA preparations was demonstrated by PCR amplification with a set of primers, each derived from the Z5 insert and from flanking sequences (*11*).

PCR amplification of genomic DNA with primers flanking the 3′ and 5′ junctions of the deletion found in the W15 clone revealed the presence of introns on both sides of the deletion (Fig. 2B). Thus, clone W15 was generated by alternative splicing and the zinc finger domain of the ARF1 GAP is encoded by a distinct exon. In addition to four cysteines, two conserved histidines that are encoded by this exon are also likely to participate in the formation of the zinc finger.

Coupled in vitro transcription and translation of the Z6 clone in a reticulocyte lysate (Fig. 3A, left panel) resulted in two ^{35}S-labeled bands. The upper band of 49 kD comigrated with the tissue-purified GAP (*11*), whereas the lower band of 43 kD appears to represent a product of initiation